New Journal of Physics
The open-access journal for physics

The distribution of $r \cdot p$ in quantum mechanical systems

Yves A Bernard and Peter M W Gill[1]
Research School of Chemistry, Australian National University, ACT 0200, Australia
E-mail: peter.gill@anu.edu.au

New Journal of Physics **11** (2009) 083015 (15pp)
Received 10 June 2009
Published 13 August 2009
Online at http://www.njp.org/
doi:10.1088/1367-2630/11/8/083015

Abstract. The position–momentum dot product ('posmom') $s = \boldsymbol{r} \cdot \boldsymbol{p}$ of a particle is a quantum mechanical observable. In principle, its density $S(s)$ can be derived from the position or momentum wavefunction using Mellin transforms but this leads to complicated integrals and it has therefore been largely neglected by the molecular physics community. However, we show that $S(s)$ can be obtained easily as the Fourier transform of the hyperbolic autocorrelation of the wavefunction. Our findings are illustrated using numerical results for various states of a harmonic oscillator, a hydrogenic ion and particles in a box.

[1] Author to whom any correspondence should be addressed.

Contents

1. Introduction

Heisenberg's uncertainty principle stipulates that, because the quantum mechanical operators for the position $\boldsymbol{r}$ and momentum $\boldsymbol{p}$ of a particle do not commute, these variables cannot be measured simultaneously and a true phase-space density $S(\boldsymbol{r}, \boldsymbol{p})$ does not exist. This fundamentally non-classical result is inconvenient for Rassolov models [1]–[8] of electron correlation, in which the Hartree–Fock Hamiltonian is augmented by a linear phase-space operator that approximates the correlation energy for a single determinant wavefunction. Therefore, in order to make progress, most of those models have resorted to the Wigner quasi-density distribution [9]

$$W(\boldsymbol{r}, \boldsymbol{p}) = (\pi\hbar)^{-3} \int \psi^*(\boldsymbol{r}+\boldsymbol{q})\psi(\boldsymbol{r}-\boldsymbol{q})\mathrm{e}^{2\mathrm{i}\boldsymbol{p}\cdot\boldsymbol{q}/\hbar}\,\mathrm{d}\boldsymbol{q}, \tag{1}$$

where $\psi(\boldsymbol{r})$ is the position wavefunction. $W(\boldsymbol{r}, \boldsymbol{p})$ has the correct marginal densities $|\psi(\boldsymbol{r})|^2$ and $|\phi(\boldsymbol{p})|^2$ (where $\phi(\boldsymbol{p})$ is the momentum wavefunction) but, as Wigner recognized, it is not necessarily positive at all points in phase space.

Fortunately, it appears that the true $S(\boldsymbol{r}, \boldsymbol{p})$ is superfluous for many Rassolov models and reduced densities contain most of the physical information that is required. In this paper, we are interested in the position–momentum dot product ('posmom')

$$s = \boldsymbol{r}\cdot\boldsymbol{p} = \frac{\mathrm{d}}{\mathrm{d}t}\left(\frac{1}{2}mr^2\right), \tag{2}$$

of a particle. It is an important dynamical quantity and the sum of the posmoms of N particles is the scalar virial. Given that knowledge of s does not imply simultaneous knowledge of $\boldsymbol{r}$ and $\boldsymbol{p}$, one sees that the uncertainty principle does not necessarily preclude the measurement of s and, indeed, it is well known [10] that s is represented by an unbounded self-adjoint operator [11] and therefore is an observable.

The posmom operator in one dimension (1D) and in the position representation is

$$\bar{s} = \frac{1}{2}(\bar{x}\bar{p} + \bar{p}\bar{x}) = -\mathrm{i}\hbar\left(\frac{1}{2} + x\frac{\mathrm{d}}{\mathrm{d}x}\right), \tag{3}$$

which yields the unitary operator on $\boldsymbol{L}^2(\mathbb{R})$

$$U_\lambda = \mathrm{e}^{\mathrm{i}\lambda\bar{s}/\hbar}, \quad \lambda \in \mathbb{R}. \tag{4}$$

U_λ scales the position and momentum wavefunctions as

$$(U_\lambda\psi)(x) = \mathrm{e}^{+\lambda/2}\psi(\mathrm{e}^{+\lambda}x), \tag{5}$$

$$(U_\lambda\phi)(p) = \mathrm{e}^{-\lambda/2}\phi(\mathrm{e}^{-\lambda}p), \tag{6}$$

and the set U_λ is called the dilation group. The operator $\bar{s}$ is the generator of dilation and has been used in a variety of fields of physics, including the spectral analysis of the Schrödinger Hamiltonian [12, 13] and in the development of scattering theory [14, 15]. More recently, $\bar{s}$ has arisen as a Hamiltonian for quantum mechanical models of the zeros of the Riemann zeta function [16]–[18] and a method for the indirect experimental measurement of s (called the hyperbolic momentum) has been proposed [17].

The posmom operator is diagonalized [19, 20] through a Mellin transform [21] and its normalized eigenfunctions $f_s^{\pm}(x)$ are defined [22, 23] on the positive and negative axes by

$$f_s^+(x) = \begin{cases} (2\pi\hbar)^{-1/2}\, x^{-1/2+\mathrm{i}s/\hbar}, & x > 0, \\ 0, & x \leqslant 0, \end{cases} \tag{7a}$$

$$f_s^-(x) = \begin{cases} 0, & x \geqslant 0 \\ (2\pi\hbar)^{-1/2}|x|^{-1/2+\mathrm{i}s/\hbar}, & x < 0. \end{cases} \tag{7b}$$

These can be rotated into even and odd functions and one can then obtain the posmom density from the position or momentum wavefunction. However, this becomes mathematically difficult in complicated systems and, as a result, the posmom has been largely overlooked in the molecular physics community. This is unfortunate because s contains physical information that is inaccessible from measurements of the position or momentum densities.

In section 2, we show that the difficulties of the Mellin transforms can be avoided by recognizing that the posmom density $S(s)$ is the Fourier transform of the hyperbolic autocorrelation of the position or momentum wavefunction. This new approach allows the facile construction of the posmom density of the electrons in molecular systems and offers fresh insights into the results of electronic structure calculations. In section 3, we illustrate this through numerical results for various states of a harmonic oscillator, a hydrogenic ion and particles in a box.

2. Theory

2.1. Posmom density

Our approach is motivated by the observation that, from the normalized eigenfunctions

$$f_\mathrm{p}(x) = (2\pi\hbar)^{-1/2}\exp(\mathrm{i}px/\hbar) \tag{8}$$

of the momentum operator

$$\bar{p} = -\mathrm{i}\hbar\frac{\mathrm{d}}{\mathrm{d}x}, \tag{9}$$

one can construct even and odd functions

$$f_{\mathrm{p}}^{\mathrm{e}}(x) = (2\pi\hbar)^{-1/2}\cos(px/\hbar), \tag{10a}$$

$$f_{\mathrm{p}}^{\mathrm{o}}(x) = (2\pi\hbar)^{-1/2}\sin(px/\hbar), \tag{10b}$$

and obtain the momentum density

$$\Pi(p) = \left|\int_{-\infty}^{\infty} f_{\mathrm{p}}^{\mathrm{e}}(x)\psi_{\mathrm{e}}(x)\right|^2 + \left|\int_{-\infty}^{\infty} f_{\mathrm{p}}^{\mathrm{o}}(x)\psi_{\mathrm{o}}(x)\right|^2 \tag{11}$$

in terms of contributions from the even and odd parts of the position wavefunction

$$\psi(x) = \psi_{\mathrm{e}}(x) + \psi_{\mathrm{o}}(x). \tag{12}$$

In much the same way, the posmom eigenfunctions (7) can be rotated into sets of even and odd functions

$$f_s^{\mathrm{e}}(x) = (4\pi\hbar)^{-1/2}|x|^{-1/2+\mathrm{i}s/\hbar}, \tag{13a}$$

$$f_s^{\mathrm{o}}(x) = \mathrm{sgn}\,(x)\; f_s^{\mathrm{e}}(x), \tag{13b}$$

and, by analogy with (11), the posmom density is then

$$\begin{aligned} S(s) &= \left|\int_{-\infty}^{\infty} f_s^{\mathrm{e}}(x)\psi_{\mathrm{e}}(x)\right|^2 + \left|\int_{-\infty}^{\infty} f_s^{\mathrm{o}}(x)\psi_{\mathrm{o}}(x)\right|^2 \\ &= \frac{|\mathcal{M}_{\mathrm{e}}(\sigma)|^2 + |\mathcal{M}_{\mathrm{o}}(\sigma)|^2}{\pi\hbar}, \end{aligned} \tag{14}$$

where we have introduced the dimensionless variable

$$\sigma = 1/2 - \mathrm{i}s/\hbar \tag{15}$$

and $\mathcal{M}_{\mathrm{e}}$ and $\mathcal{M}_{\mathrm{o}}$ are the Mellin transforms of ψ_{e} and ψ_{o} [21]. It is clear that $S(s)$ is both real and even and we will therefore restrict our attention to $s \geqslant 0$. Moreover, to simplify our formulae, we will also assume that s is measured in units of $\hbar$.

Unfortunately, the Mellin pathway (14) leads to complicated integrals, especially in higher dimensions, and historically this has hindered the routine construction of $S(s)$ in electronic structure calculations. However, in appendix A, we show that the Fourier transform

$$\hat{S}(k) = \int_{-\infty}^{\infty} S(s)\,\mathrm{e}^{-\mathrm{i}ks}\,\mathrm{d}s \tag{16}$$

of the posmom density can be cast into the form

$$\hat{S}(k) = \int_{-\infty}^{\infty} \psi^*(\mathrm{e}^{+k\hbar/2}x)\;\psi(\mathrm{e}^{-k\hbar/2}x)\,\mathrm{d}x, \tag{17}$$

or equivalently, by Parseval's theorem,

$$\hat{S}(k) = \int_{-\infty}^{\infty} \phi^*(\mathrm{e}^{-k\hbar/2}p)\;\phi(\mathrm{e}^{+k\hbar/2}p)\,\mathrm{d}p. \tag{18}$$

These beautiful equations reveal that $\hat{S}(k)$ is simply the overlap between dilated and anti-dilated versions of the position (or momentum) wavefunction and we will therefore call $\hat{S}(k)$ the hyperbolic autocorrelation.

For a particle in ν dimensions, it can be shown that

$$\hat{S}(k) = \int \psi^*(\mathrm{e}^{+k\hbar/2}\boldsymbol{r})\,\psi(\mathrm{e}^{-k\hbar/2}\boldsymbol{r})\,\mathrm{d}\boldsymbol{r}, \tag{19}$$

and these integrals are so much simpler than those in the Mellin formulation (14) that it now becomes possible to generate the posmom density $S(s)$ easily from the results of conventional electronic structure calculations on arbitrary molecular systems.

Because $\hat{S}(k)$ is both real and even, we will restrict our attention to $k \geqslant 0$. We will also assume henceforth that k is measured in units of $\hbar^{-1}$.

2.2. Many-particle systems

Posmom theory extends easily to N-particle systems, especially within independent-electron models. If the wavefunction is a (bosonic) Hartree product

$$\Psi(\boldsymbol{r}) = \mathcal{S}[\psi_1(\boldsymbol{r}_1)\psi_2(\boldsymbol{r}_2)\ldots\psi_N(\boldsymbol{r}_N)], \tag{20}$$

or a (fermionic) Slater determinant

$$\Psi(\boldsymbol{r}) = \mathcal{A}[\psi_1(\boldsymbol{r}_1)\psi_2(\boldsymbol{r}_2)\ldots\psi_N(\boldsymbol{r}_N)] \tag{21}$$

(where $\mathcal{S}$ and $\mathcal{A}$ are symmetrizing and antisymmetrizing operators) of orthogonal orbitals $\psi_j(\boldsymbol{r})$, it can be shown that the hyperbolic autocorrelation

$$\hat{S}(k) = \sum_{j=1}^{N} \int \psi_j^*(\mathrm{e}^{+k/2}\boldsymbol{r})\,\psi_j(\mathrm{e}^{-k/2}\boldsymbol{r})\,\mathrm{d}\boldsymbol{r} \tag{22}$$

is a sum of contributions from each orbital. It follows, therefore, that the density $S(s)$ is also sums of orbital contributions.

3. Examples

3.1. Harmonic oscillator

The nth state of the 1D quantum mechanical harmonic oscillator with $\hbar = m = k = 1$ and Hamiltonian

$$\bar{H} = -\frac{1}{2}\frac{\mathrm{d}^2}{\mathrm{d}x^2} + \frac{1}{2}x^2 \tag{23}$$

has the position wavefunction

$$\psi_n(x) = \frac{H_n(x)\exp(-x^2/2)}{\pi^{1/4}\sqrt{2^n n!}}, \tag{24}$$

where $H_n(x)$ are the nth Hermite polynomials [24] and the energy

$$E_n = n + 1/2. \tag{25}$$

Equation (19) yields the hyperbolic autocorrelations

$$\hat{S}_n(k) = P_n(\operatorname{sech} k)\operatorname{sech}^{1/2}k, \tag{26}$$

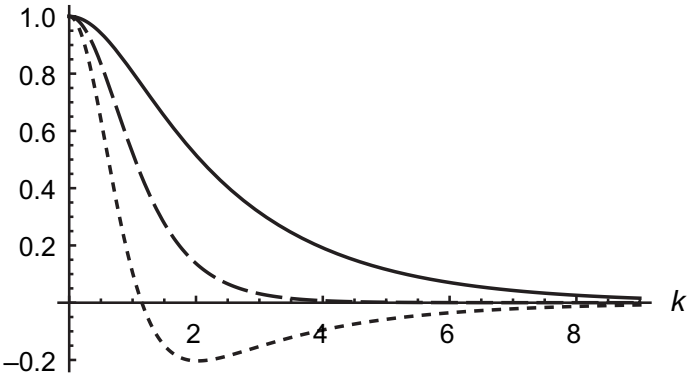

Figure 1. Hyperbolic autocorrelations $\hat{S}_0(k)$ (solid), $\hat{S}_1(k)$ (dashed) and $\hat{S}_2(k)$ (dotted) of a 1D harmonic oscillator.

where P_n is the nth Legendre polynomial [24]. In particular, the three lowest states yield

$$\hat{S}_0(k) = \operatorname{sech}^{1/2} k, \tag{27a}$$

$$\hat{S}_1(k) = \operatorname{sech}^{3/2} k, \tag{27b}$$

$$\hat{S}_2(k) = \tfrac{3}{2}\operatorname{sech}^{5/2} k - \tfrac{1}{2}\operatorname{sech}^{1/2} k, \tag{27c}$$

and these are compared in figure 1. The curves coincide at $k = 0$ because the corresponding densities are normalized. As n increases, the $\hat{S}_n(k)$ tighten around the origin. As k increases, the $\hat{S}_{2n}(k)$ and $\hat{S}_{2n+1}(k)$ decay as $O(\mathrm{e}^{-k/2})$ and $O(\mathrm{e}^{-3k/2})$, respectively.

Fourier inversion of (26) yields the posmom densities

$$S_n(s) = \frac{2^{4n}}{2^{3/2}\pi^2} \sum_{j=0}^{\lfloor n/2 \rfloor} \frac{(-1)^j}{2^{8j}} \frac{\Gamma(n-j+\frac{1}{2})}{j!(2n-4j)!} \left| \Gamma\left(\frac{n-2j+\sigma}{2}\right) \right|^2, \tag{28}$$

where Γ is the gamma function [24] and σ is defined in (15). For the lowest states, one finds

$$S_0(s) = 2^{-3/2}\pi^{-3/2} \left| \Gamma\left(\frac{\sigma}{2}\right) \right|^2, \tag{29a}$$

$$S_1(s) = 2^{1/2}\pi^{-3/2} \left| \Gamma\left(\frac{\sigma+1}{2}\right) \right|^2, \tag{29b}$$

$$S_2(s) = 2^{1/2}\pi^{-3/2} s^2 \left| \Gamma\left(\frac{\sigma}{2}\right) \right|^2, \tag{29c}$$

and these are shown in figure 2. As expected, the posmom density broadens as n increases. At $s = 0$, the densities drop from $S_0(0) \approx 0.83$ to $S_1(0) \approx 0.38$ to $S_2(0) = 0$. For large s,

$$S_0(s) \sim \pi^{-1/2} s^{-1/2} \exp(-\pi s/2), \tag{30a}$$

$$S_1(s) \sim 2\pi^{-1/2} s^{1/2} \exp(-\pi s/2), \tag{30b}$$

$$S_2(s) \sim 2\pi^{-1/2} s^{3/2} \exp(-\pi s/2), \tag{30c}$$

showing that the decay rate decreases slightly as n increases.

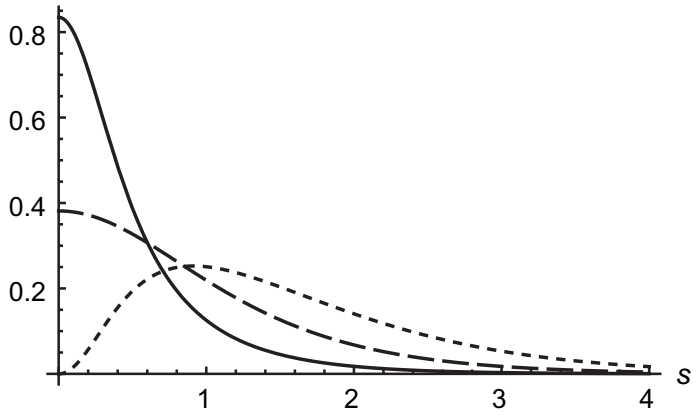

Figure 2. Posmom densities $S_0(s)$ (solid), $S_1(s)$ (dashed) and $S_2(s)$ (dotted) of a 1D oscillator.

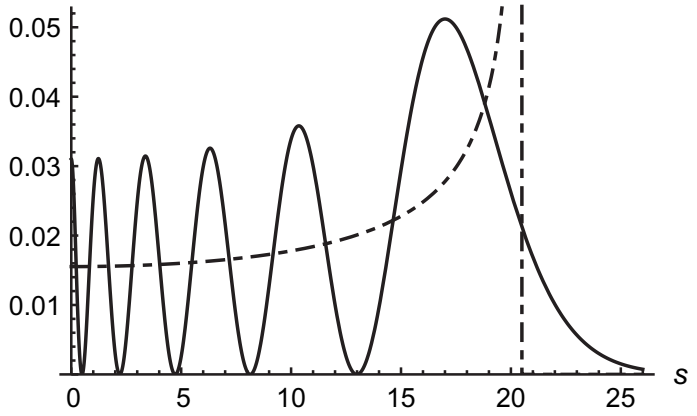

Figure 3. Posmom density $S_{20}(s)$ (solid) and the classical analog $\mathcal{P}_{20}(s)$ (dot-dash) for the $n = 20$ state of a 1D oscillator.

We now turn our attention to highly excited states and the correspondence principle. A classical oscillator with $m = k = 1$ and $E = n + 1/2$ evolves in time t as

$$x_n(t) = \sqrt{2E}\sin t, \tag{31}$$

$$p_n(t) = \sqrt{2E}\cos t, \tag{32}$$

$$s_n(t) = E\sin 2t, \tag{33}$$

and the classical time-averaged probability density for s is easily shown to be

$$\mathcal{P}_n(s) = \begin{cases} \pi^{-1}\left(E^2 - s^2\right)^{-1/2}, & s < E, \\ 0, & s > E. \end{cases} \tag{34}$$

Figure 3 compares the posmom and classical densities for the $n = 20$ state. If we ignore the fine structure, $S_{20}(s)$ clearly approaches the classical limit. The posmom density predicts that classically forbidden values of the posmom (i.e. $s > n + 1/2$) have non-vanishing probabilities.

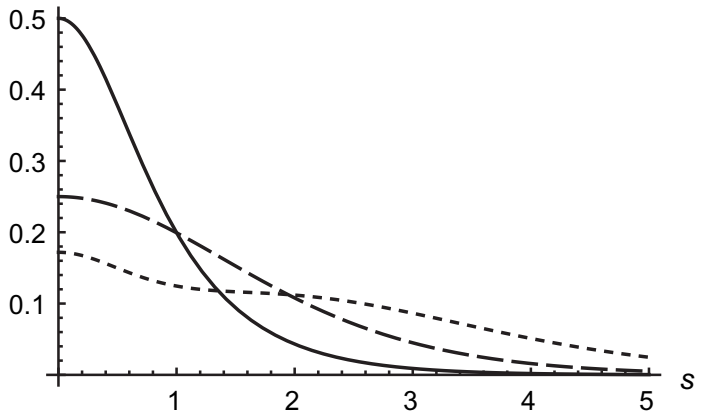

Figure 4. Posmom densities $S_{0,0}(s)$ (solid), $S_{1,1}(s)$ (dashed) and $S_{2,2}(s)$ (dotted) of a 2D oscillator.

Extensions to the harmonic oscillator in higher dimensions are not difficult because the wavefunctions, and thus the hyperbolic autocorrelations, factorize into Cartesian components. Thus, for a 2D oscillator, the hyperbolic autocorrelation is

$$\hat{S}_{m,n}(k) = \hat{S}_m(k)\,\hat{S}_n(k), \tag{35}$$

where the $\hat{S}_j(k)$ are given by (26). This yields, for example, the posmom densities

$$S_{0,0}(s) = \frac{1}{2}\operatorname{sech}\left(\frac{\pi s}{2}\right), \tag{36a}$$

$$S_{1,1}(s) = \frac{s^2+1}{4}\operatorname{sech}\left(\frac{\pi s}{2}\right), \tag{36b}$$

$$S_{2,2}(s) = \frac{3s^4+6s^2+11}{64}\operatorname{sech}\left(\frac{\pi s}{2}\right), \tag{36c}$$

and these are shown in figure 4. The ground-state density for the 2D oscillator is clearly flatter than its 1D analogue in figure 2.

By analyzing the motion of a classical harmonic oscillator in 2D (with $E_x = E_y = n + \frac{1}{2}$ and $E = E_x + E_y$), one can show that the classical time-averaged posmom density is

$$\mathcal{P}_{n,n}(s) = \begin{cases} 2\pi^{-2}E^{-1}\,K(1-s^2/E^2), & s < E, \\ 0, & s > E, \end{cases} \tag{37}$$

where K is the complete elliptic integral of the first kind [24] and figure 5 shows that the posmom density $S_{20,20}(s)$ approaches this limit quite closely.

3.2. Hydrogenic ions

The position wavefunctions

$$\psi_{nlm}(\boldsymbol{r}) = R_{nl}(Zr)Y_{lm}(\theta,\phi), \tag{38}$$

of a hydrogenic ion with nuclear charge Z factorize into radial and angular parts. Varying Z leads to a simple length dilation of the $\psi_{nlm}(\boldsymbol{r})$ and therefore has no effect on the hyperbolic

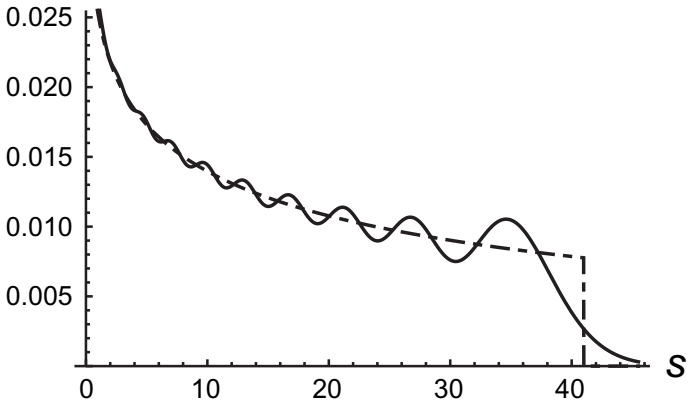

Figure 5. Posmom density $S_{20,20}(s)$ (solid) and classical density $\mathcal{P}_{20,20}(s)$ (dot-dash) for a highly excited 2D oscillator.

autocorrelations and posmom densities. Substituting equation (38) into equation (19), one finds

$$\hat{S}_{nlm}(k) = \int_0^\infty \int_0^\pi \int_0^{2\pi} R_{nl}^*(\mathrm{e}^{+k/2}r)\, Y_{lm}^*(\theta,\phi)\, R_{nl}(\mathrm{e}^{-k/2}r)\, Y_{lm}(\theta,\phi)\, r^2 \sin\theta \,\mathrm{d}r\,\mathrm{d}\theta\,\mathrm{d}\phi$$

$$= \int_0^\infty R_{nl}^*(\mathrm{e}^{+k/2}r)\, R_{nl}(\mathrm{e}^{-k/2}r)\, r^2\,\mathrm{d}r \tag{39}$$

which shows that the $\hat{S}_{nlm}(k)$ and $S_{nlm}(s)$ depend only on the radial part of the wavefunction.

Solving the integral (39) gives

$$\hat{S}_{nlm}(k) = P_{n-l-1}^{(0,2l+1)}\left(2\,\mathrm{sech}^2\frac{k}{2} - 1\right)\mathrm{sech}^{2l+3}\frac{k}{2}, \tag{40}$$

where $P_n^{(a,b)}$ is a Jacobi polynomial [24] and this yields

$$S_{nlm}(s) = Q_{nl}(s^2)\,\mathrm{sech}(\pi s), \tag{41}$$

where Q_{nl} is a polynomial. The hyperbolic autocorrelations for the three lowest states are

$$\hat{S}_{100}(k) = \mathrm{sech}^3\frac{k}{2}, \tag{42a}$$

$$\hat{S}_{200}(k) = -2\,\mathrm{sech}^3\frac{k}{2} + 3\,\mathrm{sech}^5\frac{k}{2}, \tag{42b}$$

$$\hat{S}_{210}(k) = \mathrm{sech}^5\frac{k}{2}, \tag{42c}$$

and these yield the posmom densities

$$S_{100}(s) = \tfrac{1}{2}(4s^2+1)\,\mathrm{sech}(\pi s), \tag{43a}$$

$$S_{200}(s) = \tfrac{1}{8}(4s^2+1)^2\,\mathrm{sech}(\pi s), \tag{43b}$$

$$S_{210}(s) = \tfrac{1}{24}(16s^4+40s^2+9)\,\mathrm{sech}(\pi s), \tag{43c}$$

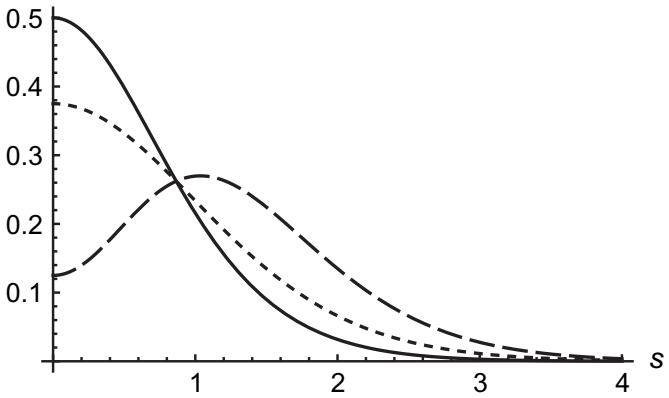

Figure 6. Posmom densities $S_{100}(s)$ (solid), $S_{100}(s)$ (dashed) and $S_{210}(s)$ (dotted) of a hydrogenic ion.

which are shown in figure 6. The radial parts of the 1s and 2p wavefunctions are nodeless and their posmom densities $S_{100}(s)$ and $S_{210}(s)$ are therefore qualitatively similar, possessing maxima at $s = 0$ and decaying monotonically as s increases. In contrast, because the 2s wavefunction has a radial node at $r = 2/Z$, its posmom density $S_{200}(s)$ is qualitatively different, rising to a maximum near $s = 1$.

3.3. A particle in a box

The wavefunctions for a particle inside a 1D box of length L centered at $x = 0$ are

$$\psi_n(x) = \begin{cases} \sqrt{2/L}\,\cos(n\pi x/L), & n \text{ odd}, \\ \sqrt{2/L}\,\sin(n\pi x/L), & n \text{ even}, \end{cases} \tag{44}$$

and their energies are

$$E_n = \frac{n^2\pi^2}{2L^2}. \tag{45}$$

Using (19), one finds the hyperbolic autocorrelations

$$\hat{S}_n(k) = j_0(n\kappa)\,\operatorname{sech}\frac{k}{2}, \tag{46}$$

where j_0 is a spherical Bessel function [24] and

$$\kappa = \frac{\pi}{1+\coth(k/2)}, \tag{47}$$

and we note that the $\hat{S}_n(k)$ are independent of L because it simply induces a dilation. The resulting posmom densities are

$$S_n(s) = \frac{1}{2n\pi^2}\left|\mathrm{i}^{n-\sigma}\gamma\left(\sigma, \frac{\mathrm{i}n\pi}{2}\right) - \mathrm{i}^{\sigma-n}\gamma\left(\sigma, -\frac{\mathrm{i}n\pi}{2}\right)\right|^2, \tag{48}$$

where $\gamma(a, z)$ is the incomplete gamma function [24].

The densities of the lowest states of particle in a box are shown in figure 7 and are remarkably similar to the analogous densities (figure 2) for the harmonic oscillator. However,

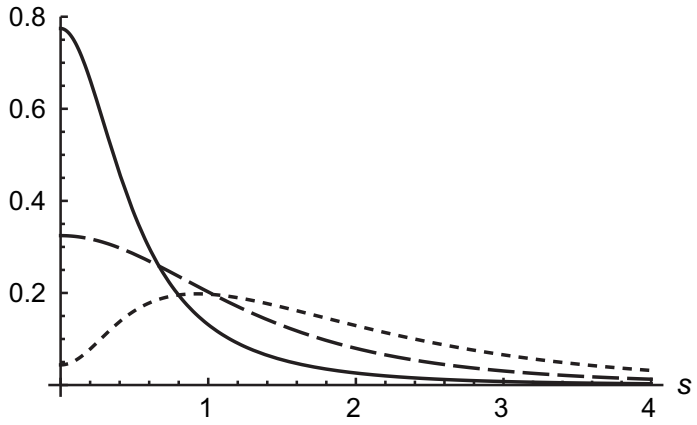

Figure 7. Posmom densities $S_1(s)$ (solid), $S_2(s)$ (dashed) and $S_3(s)$ (dotted) of a particle in a 1D box.

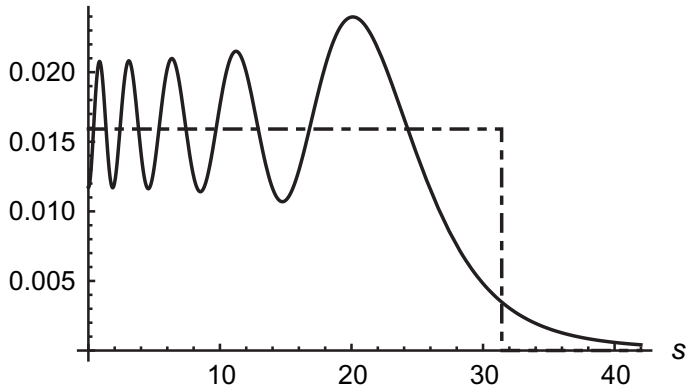

Figure 8. Posmom density $S_{20}(s)$ (solid) and classical density $\mathcal{P}_{20}(s)$ (dot-dash) for the $n = 20$ state of a particle in a 1D box.

whereas the third state of the harmonic oscillator has a node at $s = 0$, the same state of a particle in a box has $S_3(0) \approx 0.04$.

Like the harmonic oscillator, the particle in a box behaves classically when n is large. In classical mechanics, its position is uniformly distributed between $-L/2$ and $+L/2$ and, because its energy given by (45) is kinetic, its momentum $p = \pm n\pi/L$. It follows that its classical posmom density is uniformly distributed and

$$\mathcal{P}_n(s) = \begin{cases} (n\pi)^{-1}, & s < n\pi/2, \\ 0, & s > n\pi/2. \end{cases} \tag{49}$$

Figure 8 compares $\mathcal{P}_{20}(s)$ with the true density $S_{20}(s)$. Ignoring fine structure, it is clear that $S_{20}(s)$ is approaching the classical limit.

Extensions to higher-dimensional boxes are straightforward because of the same Cartesian factorization that was exploited for the harmonic oscillator. For example, the hyperbolic autocorrelation in a 2D box is

$$\hat{S}_{m,n}(k) = j_0(m\kappa)\, j_0(n\kappa)\, \operatorname{sech}^2 \frac{k}{2}. \tag{50}$$

3.4. Fermions in a box

Suppose that $2N$ non-interacting fermions occupy the lowest N orbitals in a 1D box. Then the hyperbolic autocorrelation (22) is

$$\hat{S}^{1D}(k) = 2\,\mathrm{sech}\frac{k}{2}\sum_{n=1}^{N} j_0(n\kappa)$$

$$= 2N - \left[\frac{\pi^2 N(N+1)(2N+1)}{72} + \frac{N}{4}\right]k^2 + \cdots. \tag{51}$$

The even moments of $S(s)$ are easily extracted from the derivatives of $\hat{S}(k)$ at $k = 0$ and one finds that the root-mean-square (rms) value of a particle's posmom is

$$s_{\mathrm{rms}}^{1D} = \sqrt{\frac{\pi^2(N+1)(2N+1)}{72} + \frac{1}{4}} \approx \frac{\pi N}{6}. \tag{52}$$

In a square (2D) box, the hyperbolic autocorrelation is

$$\hat{S}^{2D}(k) = 2\,\mathrm{sech}^2\frac{k}{2}\sum_{n_x,n_y} j_0(n_x\kappa)\; j_0(n_y\kappa) \tag{53}$$

where the sum is over lattice points in a Fermi quadrant. If this sum is approximated by an integral, we obtain

$$\hat{S}^{2D}(k) \approx 2\,\mathrm{sech}^2 k \int_{\pi r^2/4<N} j_0(x\kappa)\; j_0(y\kappa)\,\mathrm{d}\boldsymbol{r}$$

$$= 2N - \left[\frac{2\pi N^2}{12} + \frac{N}{2}\right]k^2 + \cdots \tag{54}$$

from which the rms posmom is

$$s_{\mathrm{rms}}^{2D} \approx \left(\frac{\pi N}{6}\right)^{1/2}. \tag{55}$$

In a cubic (3D) box, an analogous treatment yields

$$\hat{S}^{3D}(k) \approx 2\,\mathrm{sech}^3\frac{k}{2}\int_{\pi r^3/6<N} j_0(x\kappa)\; j_0(y\kappa)\; j_0(z\kappa)\,\mathrm{d}\boldsymbol{r}$$

$$= 2N - \left[\frac{6^{2/3}\pi^{4/3}N^{5/3}}{20} + \frac{3N}{4}\right]k^2 + \cdots \tag{56}$$

from which the rms posmom is

$$s_{\mathrm{rms}}^{3D} \approx \left(\frac{3\pi^2 N}{20\sqrt{5}}\right)^{1/3}. \tag{57}$$

The results in (52), (55) and (57) show that the rms posmom of a particle in a ν-dimensional Fermi gas varies as $N^{1/\nu}$. This is illustrated in figure 9, which shows $S(s)$ for 204 non-interacting fermions in 1D, 2D and 3D boxes. Whereas the posmom density in 1D is almost uniform, it decays almost linearly in 2D and becomes bell-shaped in 3D.

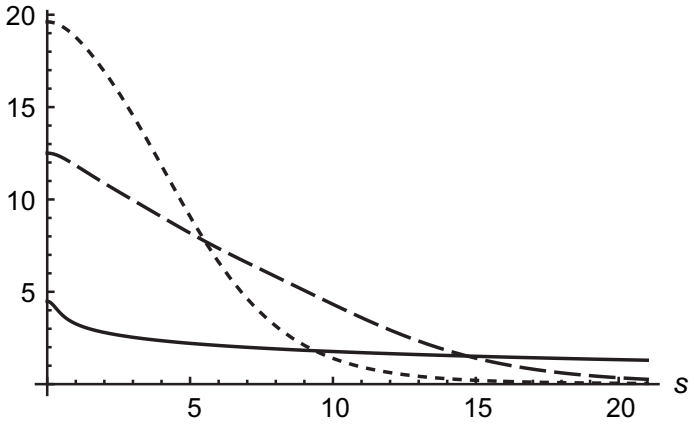

Figure 9. Posmom densities $S(s)$ of the ground state of 204 fermions in a 1D (solid), a 2D (dashed) and 3D (dotted) box.

4. Conclusion

We have shown that probability density $S(s)$ of the position–momentum dot product $s = \boldsymbol{r} \cdot \boldsymbol{p}$ is the Fourier transform of a hyperbolic autocorrelation of the position (or momentum) wavefunction and we have used this to examine $S(s)$ for a variety of quantum systems.

Posmom densities for highly excited states approach the appropriate classical densities, as expected from the correspondence principle.

The posmom density is an observable that may prove to be an informative quantity if measured experimentally and we are now performing a comprehensive study of the posmom densities of small atoms and molecules [25]. It will also be useful in future developments of electron correlation models that utilize information about both the positions and momenta of electrons.

Acknowledgments

We are grateful to Werner Amrein, Ruth Durrer, Craig Savage and John Close for stimulating discussions. YAB thanks the ANU Research School of Chemistry for a PhD scholarship.

Appendix A. Hyperbolic autocorrelation

The Fourier transform of the first term in expression (14) for the posmom density is

$$\hat{S}_{\mathrm{e}}(k) = \frac{1}{\pi} \int_{-\infty}^{\infty} |\mathcal{M}_{\mathrm{e}}(\sigma)|^2 \, \mathrm{e}^{-\mathrm{i}ks} \, \mathrm{d}s. \tag{A.1}$$

By substituting the definition of the Mellin transform and using the Dirac identity

$$\frac{1}{2\pi} \int_{-\infty}^{\infty} z^{\mathrm{i}s} \mathrm{e}^{-\mathrm{i}ks} \, \mathrm{d}s = \delta(k - \ln z) \tag{A.2}$$

to integrate over s, we obtain

$$\begin{aligned}\hat{S}_{\mathrm{e}}(k) &= \frac{1}{\pi}\int_0^\infty\int_0^\infty\int_{-\infty}^\infty \frac{u^{+\mathrm{i}s}}{\sqrt{u}}\psi_{\mathrm{e}}^*(u)\frac{v^{-\mathrm{i}s}}{\sqrt{v}}\psi_{\mathrm{e}}(v)\mathrm{e}^{-\mathrm{i}ks}\,\mathrm{d}s\,\mathrm{d}v\,\mathrm{d}u\\ &= 2\int_0^\infty\int_0^\infty \psi_{\mathrm{e}}^*(u)\psi_{\mathrm{e}}(v)\,\frac{\delta[k-\ln(u/v)]}{\sqrt{uv}}\,\mathrm{d}v\,\mathrm{d}u\\ &= 2\int_0^\infty \psi_{\mathrm{e}}^*(u)\psi_{\mathrm{e}}(\mathrm{e}^{-k}u)\mathrm{e}^{-k/2}\,\mathrm{d}u\\ &= 2\int_0^\infty \psi_{\mathrm{e}}^*(\mathrm{e}^{+k/2}x)\psi_{\mathrm{e}}(\mathrm{e}^{-k/2}x)\,\mathrm{d}x\\ &= \int_{-\infty}^\infty \psi_{\mathrm{e}}^*(\mathrm{e}^{+k/2}x)\psi_{\mathrm{e}}(\mathrm{e}^{-k/2}x)\,\mathrm{d}x. \qquad \text{(A.3)}\end{aligned}$$

Proceeding similarly, one can show

$$\hat{S}_{\mathrm{o}}(k) = \frac{1}{\pi}\int_{-\infty}^\infty |\mathcal{M}_{\mathrm{o}}(\sigma)|^2\,\mathrm{e}^{-\mathrm{i}ks}\,\mathrm{d}s \qquad \text{(A.4)}$$

$$= \int_{-\infty}^\infty \psi_{\mathrm{o}}^*(\mathrm{e}^{+k/2}x)\psi_{\mathrm{o}}(\mathrm{e}^{-k/2}x)\,\mathrm{d}x \qquad \text{(A.5)}$$

and the Fourier transform of the total posmom density is therefore given by (17), as required.

Appendix B. Quasi-hyperbolic autocorrelation

Some readers may wonder about the relationship between the exact posmom density and the Wigner distribution (1). In fact, it is possible to take the classical average of the Wigner distribution as an estimate of the posmom density, and an analogous reduction was used [4, 8] to construct the dot intracule from the Omega intracule.

Proceeding in this way, the 1D distribution

$$W(x,\,p) = (\pi\hbar)^{-1}\int_{-\infty}^\infty \psi^*(x+q)\psi(x-q)\mathrm{e}^{2\mathrm{i}pq/\hbar}\mathrm{d}q \qquad \text{(B.1)}$$

yields the posmom *quasi*-density

$$S_W(s) = \int_{-\infty}^\infty W\left(x,\,\frac{s}{x}\right)\frac{\mathrm{d}x}{|x|}, \qquad \text{(B.2)}$$

and its Fourier transform can then be recast as

$$\begin{aligned}\hat{S}_W(k) &= \int\left[\int W\left(x,\,\frac{s}{x}\right)\frac{\mathrm{d}x}{|x|}\right]\mathrm{e}^{-\mathrm{i}ks}\,\mathrm{d}s\\ &= \frac{1}{\pi}\iiint \psi^*(x+q)\psi(x-q)\mathrm{e}^{\mathrm{i}s(2q/x-k)}\mathrm{d}s\,\mathrm{d}q\,\frac{\mathrm{d}x}{|x|}\\ &= \iint \psi^*(x+q)\psi(x-q)\,\delta\left[k-\frac{2q}{x}\right]\frac{2\mathrm{d}q}{|x|}\,\mathrm{d}x\\ &= \int \psi^*\left(x+\frac{k}{2}x\right)\psi\left(x-\frac{k}{2}x\right)\mathrm{d}x. \qquad \text{(B.3)}\end{aligned}$$

In general, for a particle in ν dimensions, one can show (reintroducing the units) that

$$\hat{S}_W(k) = \int \psi^*([1+\frac{k}{2}\hbar]\boldsymbol{r})\,\psi([1-\frac{k}{2}\hbar]\boldsymbol{r})\,\mathrm{d}\boldsymbol{r} \tag{B.4}$$

and comparison of this with (19) and the exponential series

$$\exp\left(\pm\frac{k}{2}\hbar\right) = 1 \pm \frac{k}{2}\hbar + \cdots \tag{B.5}$$

reveals that $\hat{S}_W(k)$, obtained from a classical average, is a first-order approximation to $\hat{S}(k)$. Thus, the quasi-density is correct to $O(\hbar)$ and becomes exact in the classical limit $\hbar \to 0$.

References

[1] Rassolov V A 1999 *J. Chem. Phys.* **110** 3672
[2] Fondermann R, Hanrath M, Dolg M and O'Neill D P 2005 *Chem. Phys. Lett.* **413** 237
[3] Besley N A 2006 *J. Chem. Phys.* **125** 074104
[4] Gill P M W, Crittenden D L, O'Neill D P and Besley N A 2006 *Phys. Chem. Chem. Phys.* **8** 15
[5] Fondermann R, Hanrath M and Dolg M 2007 *Theor. Chem. Acc.* **118** 777
[6] Dumont E E, Crittenden D L and Gill P M W 2007 *Phys. Chem. Chem. Phys.* **9** 5340
[7] Crittenden D L, Dumont E E and Gill P M W 2007 *J. Chem. Phys.* **127** 141103
[8] Bernard Y A, Crittenden D L and Gill P M W 2008 *Phys. Chem. Chem. Phys.* **10** 3447
[9] Wigner E 1932 *Phys. Rev.* **40** 749
[10] Wess J 1960 *Nuovo Cimento* **18** 1086
[11] Amrein W O 2009 *Hilbert Space Methods in Quantum Mechanics* (Lausanne: EPFL Press)
[12] Aguilar J and Combes J M 1971 *Commun. Math. Phys.* **22** 269
[13] Balsley E and Combes J M 1971 *Commun. Math. Phys.* **22** 280
[14] Jensen A 1981 *Commun. Math. Phys.* **82** 435
[15] Pearson D B 1988 *Quantum Scattering and Spectral Theory* (London: Academic)
[16] Berry M V and Keating J P 1999 *SIAM Rev.* **41** 236
[17] Twamley J and Milburn G J 2006 *New J. Phys.* **8** 328
[18] Sierra G 2008 *New J. Phys.* **10** 033016
[19] Itzykson C 1969 *J. Math. Phys.* **10** 1109
[20] Moses H E and Quesada A F 1974 *J. Math. Phys.* **15** 748
[21] Debnath L and Bhatta D 2007 *Integral Transforms and their Applications* (Boca Raton, FL: Chapman and Hall)
[22] Mourre E 1979 *Commun. Math. Phys.* **68** 91
[23] Bollini C G and Giambiagi J J 1991 *Frontier Physics—Essays in Honour of Jayme Tiomno* p 138
[24] Abramowitz M and Stegun I E 1972 *Handbook of Mathematical Functions* (New York: Dover)
[25] Bernard Y A, Crittenden D L and Gill P M W in preparation